ORIGINAL PAPER

Improving the dynamic behaviour of historic buildings using experimental data: application to a Baroque church

Rosario Ceravolo[1,2] · Erica Lenticchia[1,2] · Gaetano Miraglia[1,2] · Linda Scussolini[1]

Abstract

Vibration-based Structural Health Monitoring represents an efficient and reliable tool to build models that can predict the dynamic behaviour of heritage structures for, but not limited to, monitoring purposes. Indeed, built heritage consists of unique structures often characterized by high fragility, and the design of interventions implies several challenges, also related to restrictions on the application of modern regulations. In this context, the corroboration of the mechanical model should accompany the entire process, from design to implementation, with test campaigns performed before and after the strengthening operations to assess their effectiveness. Thus, the work presents the experimental process used for the tailoring of the seismic upgrading interventions on the church of Santa Caterina, in Casale Monferrato. More recently, the model has been updated with the results acquired from a permanent monitoring system installed in 2022, following the interventions, hence allowing assessments of their effectiveness.

Keywords Vibration-based structural health monitoring · Architectural heritage · FE model calibration · Seismic upgrading · Strengthening interventions

1 Introduction

When dealing with masonry heritage structures, the design of targeted and efficient strengthening interventions is crucial to their preservation. In general, preventive actions are preferable to post-event securing actions on structures damaged by extreme and unforeseeable events, such as earthquakes. A key aspect is that post-damage recovery interventions are often more challenging and could deal with the loss of original portions of the damaged heritage, as well as not being economically favourable. Moreover, the assessment of historical buildings is more complex than the one of ordinary structures. Heritage structures are usually characterized by an intrinsic complexity due to their transformations over centuries, the possible damage they already

suffered in the past, and other sources of uncertainties that challenge both their diagnosis and restoration. Moreover, they are often made of unique elements, and characterized by different structural and construction techniques. As a consequence, only an accurate knowledge of the asset can lead to a reduction of uncertainties in the evaluation of its structural behaviour—the geometry, the construction details, the material properties. As also stated by the ICOMOS- ISCAR-SAH principles, an accurate anamnesis stage is a crucial step when dealing with historical structures, especially in the view to design the most suitable remedial measures to preserve it. This is accomplished in the notion of minimum intervention, defined as "the intervention that optimally combines compliance with structural standards with protection and enhancement of historical value and respect for the authenticity of the structure, as far as possible" [1].

Vibration-based structural health monitoring (SHM) techniques can exploit ambient vibration noise to provide useful information on the global dynamic behaviour of a structure. These approaches are nowadays well-established in the field of SHM applied to civil structures [2]. They can rely on efficient system identification algorithms, which aims at extracting information about the attitude of the structure to respond to dynamic loading. More generally, ambient

✉ Linda Scussolini
  linda.scussolini@polito.it

1 Department of Structural, Building, and Geotechnical Engineering, Politecnico di Torino, Corso Duca degli Abruzzi 24, 10129 Turin, Italy

2 Responsible Risk Resilience Interdepartmental Centre (R3C), Politecnico di Torino, Corso Duca degli Abruzzi 24, 10129 Turin, Italy

Springer

vibration tests are an effective investigative tool: they allow the integrity of the material to be preserved as a result of their non-invasiveness and non-destructiveness, fundamental for heritage buildings, while providing low-cost information on possible variations, even pathological ones, of the dynamic response [3].

A comprehensive number of applications of vibration-based SHM to heritage buildings can be found in the literature [4–8]. In particular, this technique was mainly used to: (i) understand the structural behaviour of a building, by recording the phenomena that may influence the structural behaviour [9–11]; (ii) to calibrate numerical models that can provide realistic interpretations of the structural and seismic behaviour [4, 12, 13]; (iii) to monitor the evolution of potential damage [14–17] and the effect of human and/or environmental phenomena [18, 19]. However, vibration-based techniques can also be employed for assessing the efficacy of structural or seismic interventions, by comparing the dynamic properties (i.e. natural frequencies and mode shapes) before and after structural restoration works. Moreover, the data from monitoring systems can be crucial in the planning of new strengthening and retrofitting interventions [20, 21].

For historical buildings, also in the absence of a significant hazard level, it is particularly important to check the effectiveness of restoration and strengthening interventions over time [20, 22–24]. However, when compared with the other applications, only some examples already exist in literature on the application of vibration-based techniques to heritage structures before and after strengthening interventions: in particular, these studies involved very slender structures, such as bell towers [25, 26] and minarets [27, 28], and arched structures, such as vaults [29–31]. These studies refer mainly to towers, or parts of historical buildings, such as arches, which are often attributable to simple structural types, and therefore allowing a more straightforward interpretation of the results. However, the interpretation of the results before and after interventions becomes a non-trivial task in the case of more complex structural typologies, such as churches.

It is worth specifying here that methods based on the vibrations still show important limitations in detecting the effectiveness of some intervention techniques, which are common precisely in historical and monumental buildings, such as, for example, tie rods [32] or other elements made of high-resistance materials, which therefore modify little or no global dynamic behaviour of the structure. Other techniques (such as grout injections or reinforced repointing) can instead influence the dynamics of masonry buildings so that the improvement can be appreciated using dynamic measurements.

In this context, the development of accurate models which could properly predict the behaviour of heritage structures, allowing their preservation, and evaluating the effects of retrofit and upgrading intervention is crucial. Indeed, such buildings may present both complex spatial configuration and damage state. The construction of calibrated models may be useful to not only assess the actual state of the structure, but even identify the proper strategies of intervention. In fact, when models are specifically conceived to assimilate data obtained from vibration-based tests, they can be calibrated to fit the dynamic properties, and to make a prediction on the actual response of the building to external actions. Therefore, by combining experimental data and models, it is possible to investigate the effectiveness of interventions by making a comparison before and after their application.

The present work deals with the problem of comparing vibration characteristics before and after strengthening interventions in structures of great dynamic complexity. The final objective of this study is to define a rationale for exploiting dynamic investigation campaigns in the conception of interventions on historical and monumental structures and in verifying the improvement actually produced on their dynamic behaviour.

The present study is necessarily developed around a real-world application. The case study is the Church of Santa Maria delle Grazie, better known as Santa Caterina, in Casale Monferrato (Alessandria), Italy, which represents one of the most important examples of baroque religious architecture of its territory. Throughout the years, the church of Santa Caterina has been subjected to several investigations. An extensive dynamic campaign, which resulted in the updating of a preliminary FEM of the church, was carried out in September 2010 [3]. The experimental campaign shed light on the high vulnerability of two distinctive elements of the church, viz. the lantern and the façade. Starting from 2019, the church has been interested by an extensive preservation campaign, also comprehending the strengthening interventions on the lantern (2021) and on the façade (2022).

The paper is structured as follows. Section 2 starts by introducing the case study, focusing on historical information and the damage state before the retrofitting and preservation campaign. Furthermore, the extensive test campaign carried out in 2010, and the linear dynamic identification process and results are presented. The data are then processed and used for the calibration of the reference model. The design of the strengthening interventions is reported in Sect. 3, together with their simulation in the mechanical model. Section 4 shows the results of the new model updating based on the dynamic test campaign carried out in December 2022, i.e., after the implementation of the interventions, as well as the dynamic identification results. The modifications brought about by the interventions on the global dynamic behaviour are then discussed in Sect. 5. Conclusions are finally drawn in Sect. 6.

2 Corroboration of the reference model for the church of Santa Caterina in Casale Monferrato

2.1 Description of the case study

The church of Santa Maria delle Grazie in Casale Monferrato, better known as Santa Caterina, represents an important example of baroque religious architecture [3]. Originally designed for the Dominican nuns of Santa Caterina, after receiving her marquis palace as a gift from the Marquise Anna d'Alençon, construction was begun in 1718 and completed around 1725, becoming an example of a double-hall convent church. The main body of the church (here called the church to simplify the terminology) has an oval plan, and on the east side of the presbytery, there is the choir. The drum − dome system, characterized by an oval plan with a long-axis and a short-axis of 14 m and 10 m length, respectively, is supported by eight large columns standing in the central room. The drum stands at a height of 13 m and is 7 m tall. The oval dome is 9 m tall, has eight ribs, and is coated with a thin coating of copper plates that are directly attached to the external masonry. A lantern stands over the dome, at approximately 26 m from the ground floor. The latter has a height of 6 m and presents eight slender masonry columns. The main façade, which faces Piazza Castello, is 19 m tall, with the top part overhanging by approximately 6 m. The building is depicted in Fig. 1.

Since water infiltrations in the roofing system of the dome caused an extensive damage all over the frescos and the decorations of the dome, which led to a series of inspections. The campaign involved an exhaustive survey of the damage state. In greater detail, a cracking state of the entire structure was reconstructed through photographic surveys and laser scanning. This investigation confirmed the presence of important crack patterns in the area of the lantern and the façade.

As regards the lantern, the masonry had an evident detachment of the plaster due to the continuous water infiltration. Moreover, several horizontal cracks, both coplanar and dislocated (Fig. 2a, b), were detected on the small columns, possibly resulting in the reduction of the tensile strength of the masonry. Also, the lantern presented a horizontal crack involving the entire surface, and two cracks in sub-horizontal directions, in addition to a sub-vertical crack. On the other hand, the façade presented a visible crack, starting from the main entrance, in the vertical direction (Fig. 2c–e). These findings led to preservation interventions that started in 2019.

2.2 FE model updating based on 2010 dynamic test campaign

This extensive campaign of surveys resulted in the construction of a geometric, first, and a mechanical, then, model of the structure (Fig. 3). As can be seen, the model is made up of a limited number of macro-elements in which the material is assumed to be homogeneous, in order to allow subsequent model updating on the basis of test results. The choice of macro-elements was carried out above all on the basis of intrinsic constructive and structural homogeneity, as verified during the surveys, and the subdivision proposed by [33].

The material was modelled as linear elastic and isotropic, in this phase assumed homogeneous throughout the structure, with an elastic modulus equal to 2500 MPa, a Poisson ratio equal to 0.40, and a density of 2000 kg/m^3. The mesh was created employing mono-dimensional and bi-dimensional elements. Going into greater detail, a 2-nodes beam element with 6 DOFs at each node was chosen for the thick columns at the base, the thin columns of the lantern, and the ribs of the drum − dome system, and a 4-nodes shell element with 6 DOFs at each node for the arches and the walls composing the base, the façade, the lantern, the drum − dome system, and the external walls. The structure was assumed to be clamped at the base, and soil − structure interaction was neglected. Furthermore, because there was insufficient information available for the choir, the external walls in the model were interrupted and clamped at the edges so that the stiffness of the connection could subsequently be calibrated (the elastic modulus was initialized at 5000 MPa). This preliminary FEM was used to identify the structural portions and elements that have the greatest influence on the dynamics of the structure, both in terms of local and global behaviour, in order to properly design a setup for consequent dynamic campaigns.

A comprehensive dynamic testing campaign was carried out on the 23rd, 24th, 27th, 28th, and 29th of September 2010, with the aim of identifying the dynamic behaviour of the structure. The dynamic tests setups were designed to maximize the spatial resolution of the experimental mode shapes. Different measure setups were designed to obtain a comprehensive amount of information and to predict on time possible critical aspects. Three setups were designed to obtain the mode shapes in the three main directions (viz. translation in the x direction, translation in the y direction, and rotation around z). Each of the three setups presented 18 acquisition channels. A fourth setup was designed to link the channels during the signal processing phase. In particular, the setups are composed as follows: (i) the first one, named Dome YZ, analyse the section parallel to the plane YZ in orthogonal direction to the principal axis of the structure (Fig. 4a); (ii) the setup named Dome XZ, analyse the section parallel to the XZ plane in parallel direction to
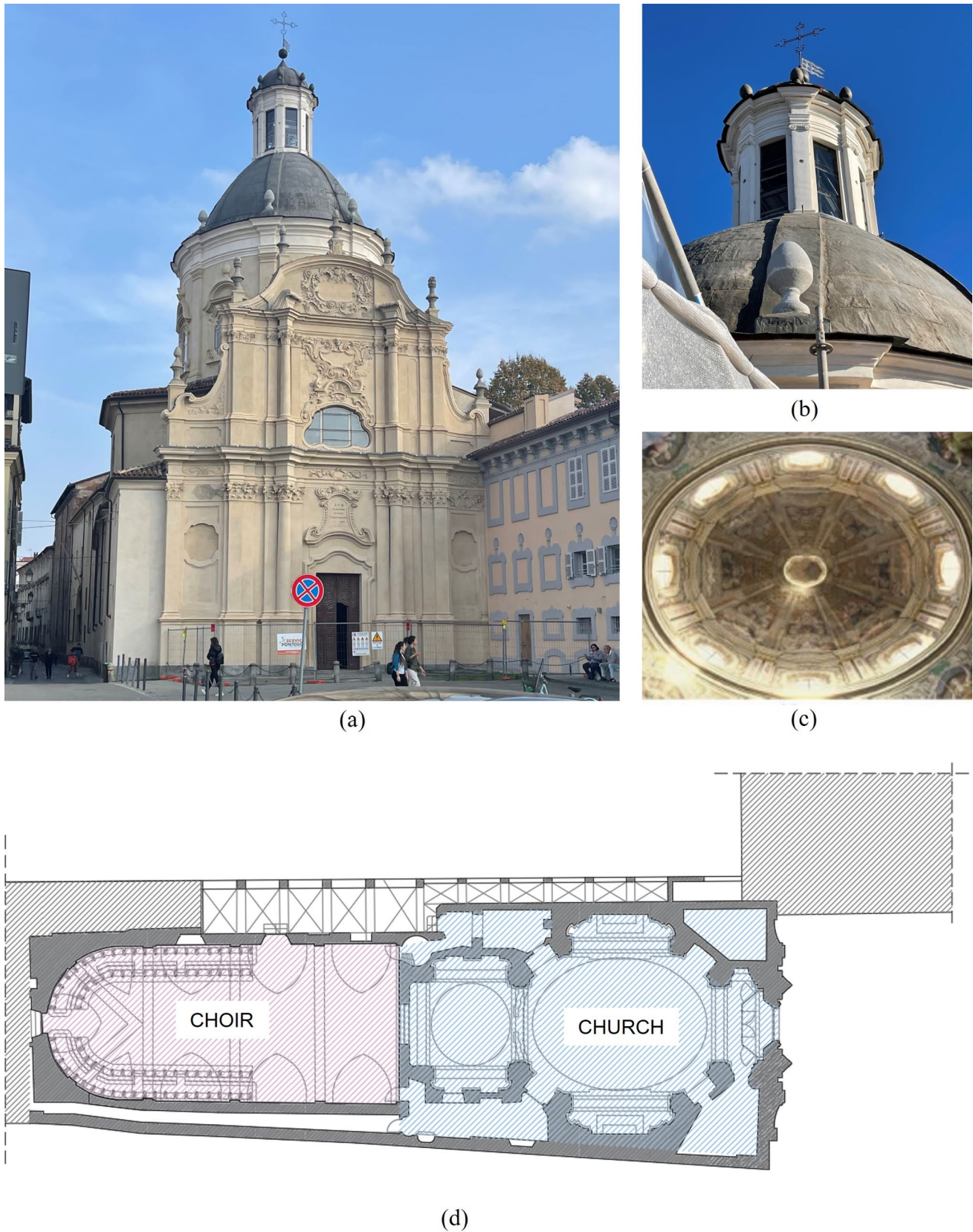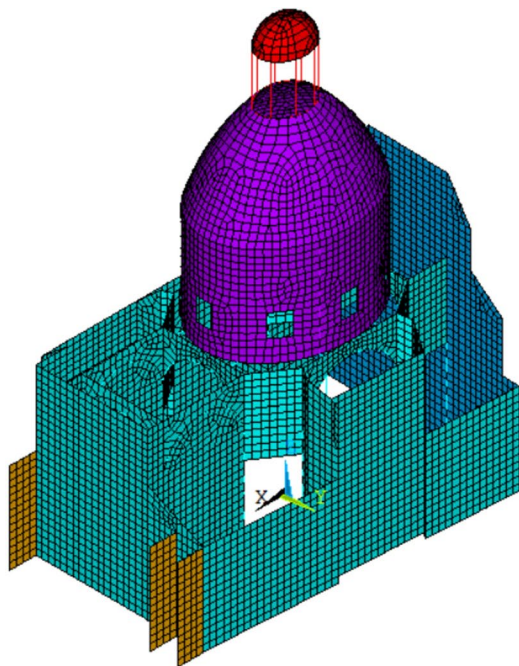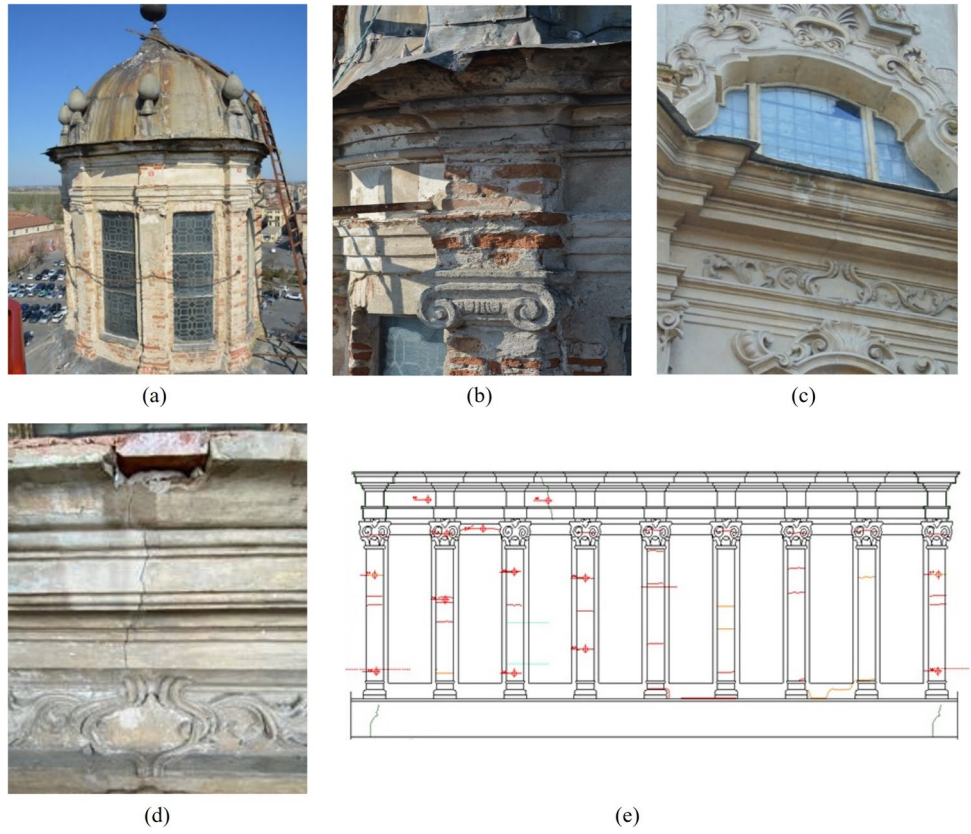
(a)

(b)

(c)

(d)

Fig. 1 General view of the Church of Santa Caterina: the façade (**a**), a detail of the lantern (**b**), internal view of the drum − dome system (**c**), and general plan of the church and the choir (**d**)

Fig. 2 Damage state of the lantern (**a**, **b**), the façade (**c**, **d**), and crack pattern of the lantern (**e**)

(a)

(b)

(c)

(d)

(e)

Macro-element	Colour
Basement	
Drum-dome system	
Lantern	
Façade	
External walls	

Fig. 3 Mechanical model of the Church of Santa Caterina with related macro-elements
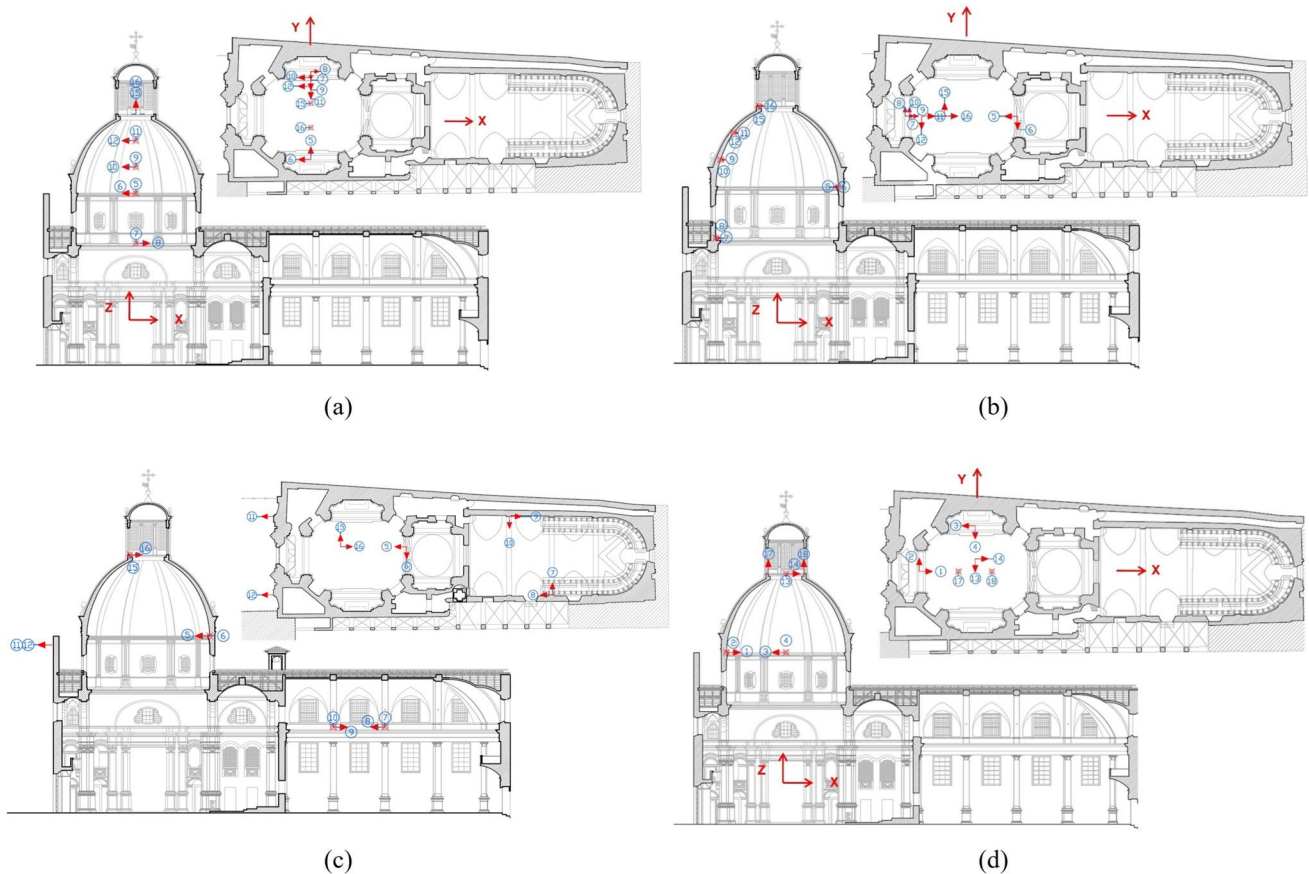
Fig. 4 Setups of the test campaign of 2010: Dome YZ (**a**), Dome XZ (**b**), Global (**c**), and Link (**d**)

the principal axis of the structure (Fig. 4b); (iii) the setup named Global, is also extended to the choir and the tympanum of the façade (Fig. 4c); (iv) while the setup named Link, is always online, allowing the combination of the various acquisitions (Fig. 4d).

The sensors used for the dynamic tests were accelerometers PCB 3701G3FA3G with a mass of 17.5 g, a sensitivity of 1 V/g, and a resolution of 30 μg. The sampling frequency was chosen to capture the response of the main vibration modes of the structure, and the signals were acquired at a sampling frequency of 400 Hz, which corresponds to a useful band spanning from 0 to 200 Hz (according to the Nyquist criterion), while the main modes were confined to 20 Hz. The acquired signals were generated by ambient excitation.

The next step was to identify the modal properties of the system under unmeasured ambient vibration excitation, thus in output-only conditions [34]. The linear dynamic identification of the structure, in terms of frequencies, mode shapes, and damping ratios, was carried out in the time domain. The technique used was the third algorithm considered by the unifying theorem of Van Overschee and De Moor [35]. This method, which is often referred to as "Canonical Variate

Analysis" (CVA), was originally developed by Larimore [36].

To maximize the information which could be extracted, the following steps were carried out: (i) uninterrupted acquisition of 20 min, corresponding to 480.000 samples at 400 Hz; (ii) filtering, de-trending, and sub-sampling; (ii) statistical analysis of the results in order to differentiate the actual modes of the structure from the modes which appear occasionally. Six main modes resulted from the identification process, as reported in Table 1. With the setups organized as reported in Fig. 4, it was possible to identify and classify all the global modes. Indeed, dynamic tests are an efficient and widely employed tool to assess inaccessible structural parts. Further details on the 2010 dynamic test campaign, including the modal shapes identified, can be found in [3].

Then, the model updating was carried out by tuning the preliminary FEM, exploiting the mode shapes and the natural frequencies extracted from the identification process. An updated model is a predictive model, which, being representative of the real structure, results in being useful as a diagnostic tool for static and seismic safety assessment and as support for the design of upgrade interventions of

Table 1 Experimental values of the first six identified natural frequencies, *f*, and damping ratios, *ζ*, from the 2010 dynamic test campaign

Identifier	Description	f [Hz]	ζ [%]
1	Transverse global mode in y direction in-phase with the dome. The lantern moves transversally (*y* direction)	3.03	1.93
2	Local façade mode. Small movements of the lantern	3.33	0.63
3	Transverse mode in y direction with torsional components and chorus, counter-phase to the dome. The lantern moves mainly transversally (*y* direction)	3.98	4.23
4	Longitudinal global mode in x direction of the drum − dome system. The lantern moves mainly longitudinally (*x* direction)	4.40	3.17
5	Transverse mode in *y* direction with high components of the lantern. The lantern moves transversally (*y* direction)	5.11	3.14
6	Torsional global mode and chorus in counter-phase to the dome	5.39	0.86

The description, instead, is inferred by using the FE model

Table 2 Results of the calibration process: frequencies obtained from the FE model vs. frequencies obtained from the dynamic identification from 2010 campaign

Identifier	Mode number in FEM (2010)	Freq. FEM (2010) [Hz]	Freq. ID. (2010) [Hz]	ΔF [%]
1	1	2.94	3.03	2.97
2	2	3.53	3.33	− 6.01
3	3	4.27	3.98	− 8.06
4	4	4.33	4.40	2.27

Table 3 Results of double flat jack tests on the masonry of the basement

Secant elastic modulus of masonry of the basement [MPa]

Nr. of trial	Range of variation of stress level [MPa]				
	[0.4–0.8]	[0.8–1.2]	[1.2–1.6]	[1.6–2]	[2–2.4]
1	2083	1333	952	909	500
2	2026	1811	1182	1270	811
3	1778	2051	1739	1538	1159

the structure. The calibration process results are reported in Table 2, which compares the first four natural frequencies resulting from the identification process and those resulting from the updated model. It is worth specifying that, in hindsight, the calibrated model also predicts a local façade mode at 2.87 Hz, which, as such, does not have many recurrences in signals.

The updated model highlighted a significant deformability of two main elements, the façade and the lantern. Indeed, the mode shapes of the updated model showed a prominent anomalous deformability of these two elements. This state of damage was confirmed by the visual inspections: the cracks in the small columns of the lantern and all over the top part of the façade, and in general their degradation, gave evidence to these results. On the other hand, the calibration of the model of the basement and the drum − dome system did not show any significant changes.

The values of the elastic modulus of the basement were confirmed by mechanical tests carried out in 2012 by using double flat jacks, and here reported in Table 3 [37]. The masonry samples were subjected to several loading and unloading cycles up to a maximum stress level of 0.8, 1.6, and 2.4 MPa, keeping the bed load value equal to 0.2 MPa. The secant elastic modulus has been calculated in the first phase of loading of each cycle. Whereas Table 3 shows the secant elastic moduli measured statically, therefore lower than the dynamic ones; moreover, although limited to a

small portion of the church, these tests only confirm the reliability of the reference mechanical model.

The mechanical tests, together with the visual inspection, allowed the characterization of the materials of the church. In particular, as observable from Table 3, and accordingly to the Italian current standards [38], a solid brick masonry can be assigned to the basement.

3 Design of the strengthening interventions

3.1 Structural interventions

The visual inspections, the definition of the damage state through an accurate crack pattern, and the experimentally updated mechanical model, highlighting a prominent deformability of lantern and façade, have further emphasized the significant vulnerability of the façade and the lantern rather than the basement and the drum − dome system, which already resulted from the simplified mechanism schemes. Therefore, strengthening solutions for both the lantern and the façade were designed using the calibrated model.

In the case of the lantern, the intervention consisted of sixteen *L*-shaped profiles with uneven sides along the columns, aligned with the interior corners of the windows. As a result, each column features two metal uprights. In addition, three *C*-shaped profiles were installed in correspondence of the windows and connected to the sidewalls using

countersunk screws. The system, as described, works as a circled cage inside the lantern, favouring a global behaviour, and is represented in Fig. 5.

The chosen material was structural steel, due to its high resistance to atmospheric conditions. In particular, S275JR steel was used for the *L*-shaped profiles and stainless steel for the plate. The risk of galvanic corrosion does not incur since hexagonal bolts were used to link the several profiles, avoiding direct contact between the different materials.

In the case of the façade, the intervention consisted in a metal frame properly connected to the tympanum (viz. the cantilever portion of the façade). The frame is characterized by tie-rods, inclined props (which work as struts or tie rods depending on the direction of the seismic action) and vertical uprights, designed to prevent the out-of-plane overturning of the masonry walls. In this case, the tympanum-frame system behaves similarly to a parallel collaborating system: the metal frame, which has a greater tensile strength, cooperates to increase the compressive strength of the masonry, without significantly modifying the stiffness and the mass distribution of the façade. Furthermore, the frame transfers and redistributes the horizontal seismic actions, thus reducing the value of the seismic response in both in-plane directions.

All the metal profiles used are made of galvanized steel S235 JR. Chemical connectors were used to link the metal frame to the masonry wall of the tympanum to simulate the behaviour of a parallel collaborating system. The chosen chemical anchor is composed by the injection cartridges of chemical resin. The connectors were positioned between the wing of the vertical uprights and the masonry within a strip 2.50 m long. A schematic representation of the connectors can be found in Fig. 6.

The systems installed on the lantern and on the façade are reported in Fig. 7.

3.2 Mechanical model accounting for the upgrading interventions

Hence, the structural interventions were introduced in the mechanical model described in Sect. 2.2 with the purpose to perform a further updating based on monitoring data acquired after the implementation of the seismic upgrading (Fig. 8).

Again, mono-dimensional, and bi-dimensional elements were employed to perform the mesh in the mechanical model of the strengthened structure. In particular, a 2-nodes beam element with 6 DOFs at each node was used for the thick columns at the base, the thin columns of the lantern, the ribs of the drum − dome system, the steel profiles on the façade and the steel profiles on the lantern, and a 4-nodes shell element with 6 DOFs at each node was used for the
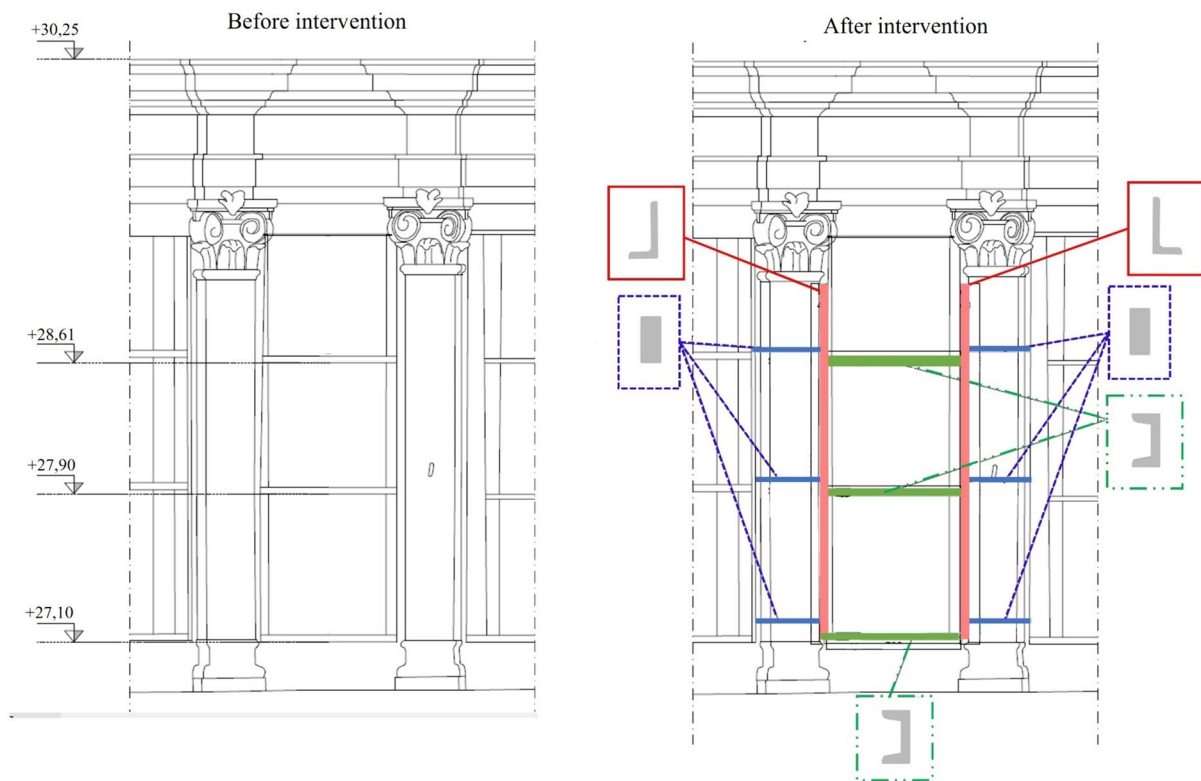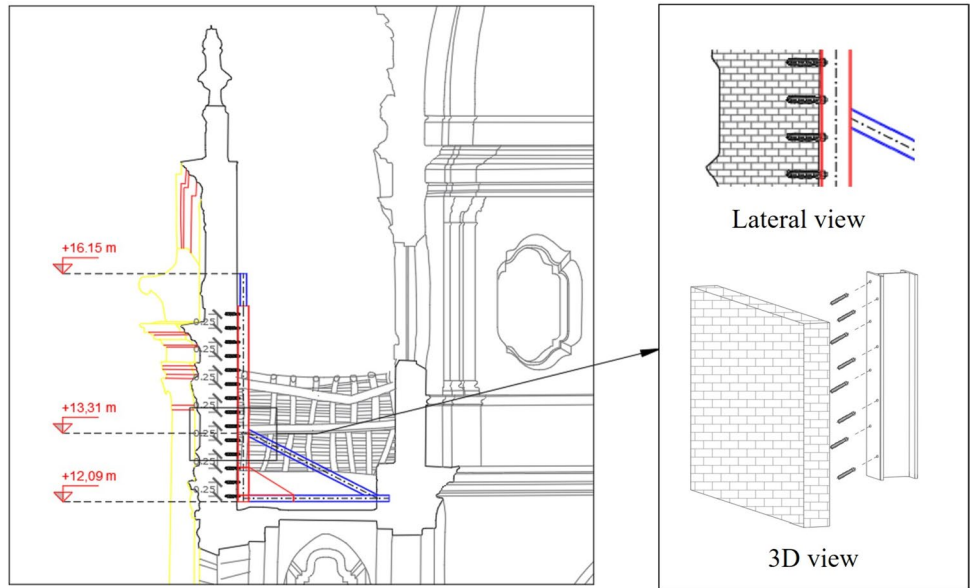

Fig. 5 Details of the lantern before and after the intervention with the corresponding profiles

Fig. 6 Details of the connection between metal frame and masonry façade
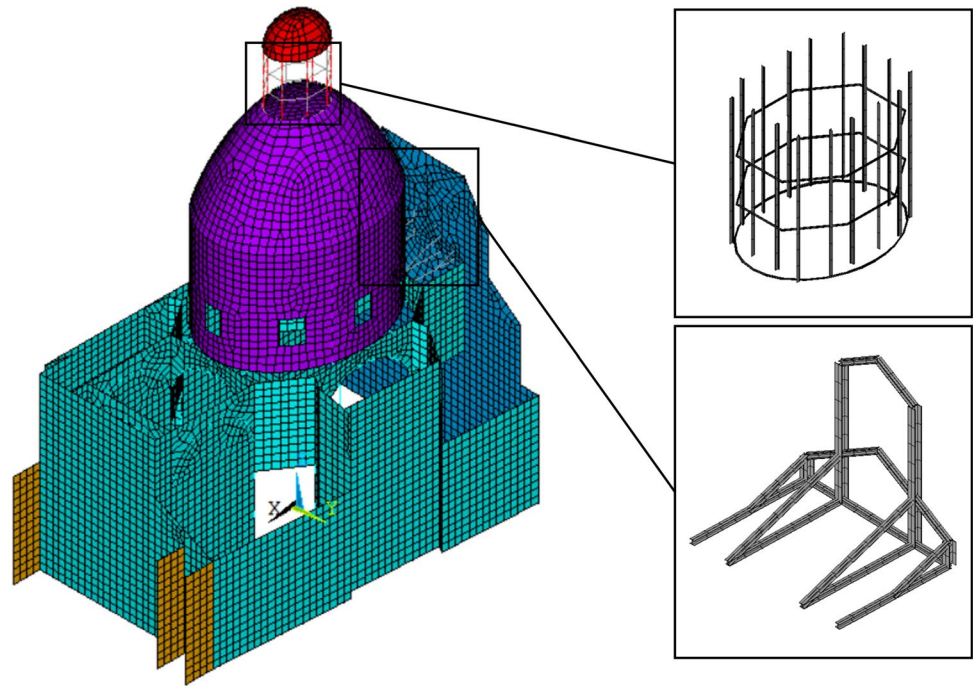

Fig. 7 Installed intervention on the lantern (**a**) and on the façade (**b**)

Fig. 8 FE model with interventions on the lantern and on the façade

arches and the walls composing the base, the façade, the lantern, the drum − dome system, and the external walls. For what concerns the materials, in the case of the masonry the values of the mechanical characteristics assumed in the preliminary mechanical model were considered. In the case of the steel, a linear elastic isotropic constitutive law with an elastic modulus of 210000 MPa, a density of 7900 kg/m^3 and a Poisson's ratio equal to 0.3 was employed. As done previously, the structure was assumed to be clamped at the base and soil − structure interaction was neglected. Moreover, the external walls linking the church to the choir and to the other adjacent buildings were modelled as laterally fixed, thus relying on the subsequent calibration of the material parameters associated with the connection walls. Finally, the frame and the façade and the cage and the lantern have been modelled as perfectly bonded linear contacts, to reflect the presence of specifically designed connectors between masonry and steel elements.

4 Results of the tests conducted after the implementation of the seismic upgrading

4.1 Dynamic tests campaign

Between December 2022 and March 2023, a permanent acquisition system acquired the ambient vibrations of the lantern of the church. The experimental tests were designed in order to extract the modal parameters of the structure, following the same output-only procedure described in the 2010 test campaign. The permanent monitoring system has two main objectives: first, collecting continuous records in order to appreciate the wandering of modal parameters for the entire duration of the experiments (December 21, 2022–March 27, 2023) so as to be able to correlate, in the future, the modal parameters (i.e. natural frequencies) with other variables that can affect their fluctuations; second, the design of a customized permanent dynamic monitoring system, covering the lantern, the façade, and other critical elements.

The experimental setup, in this case, consists of three accelerometers (i.e., high sensitivity seismic accelerometer, ceramic shear ICP® 393B12 model, 10 V/g, 0.15 to 1 k Hz, 2-pin top connection) placed on top of the lantern and positioned with the purpose of detaining the lateral and torsional vibrations of the top of this structural component. Two accelerometers were installed to acquire the accelerations in the transverse directions of the lantern, and the third one was placed to acquire its longitudinal accelerations. The generated setup is obviously sparse, making it suitable for tracking the main modal frequencies of the structure (rather than estimating the mode shapes) and assisting in the design of a future permanent monitoring system. The system records analog data that are conveyed via three-channel cables to a Dewesoft® acquisitor (viz. KRYPTON-4xACC, four channel single ended Krypton slice for Voltage, IEPE) performing signal conditioning (e.g., attenuation of electrical/thermal disturbances and anti-aliasing filter), synchronization, and signal translation from analog to digital format. The

length of the coaxial cables is 3 m. The data, once translated, are sent in digital format to a computer via a 10-m-long data cable. Inside the computer, an automatic procedure saves the data in continuous 10-min packets, referring to an absolute time. The data packets are saved on an online server and automatically stored on a computer located in the Earthquake Engineering and Dynamics laboratory (EED lab) of the Politecnico di Torino. In such manner, data are made available for further analyses. The sampling frequency used for the acquisitions is 100 Hz. Figure 9 depicts the acquisition system with sensors and the layout of the experimental setup, while the channel data of the setup are reported in Table 4.

4.2 Structural identification

A linear dynamic identification of the church of Santa Caterina was then carried out employing the acquisitions of December 22, 2022. The time frame used was the one that goes from 09:03:05 a.m. CET to 10:13:05 a.m. CET

for a total duration of the acquisitions equal to one hour and 10 min. The sampling frequency used was equal to 100 Hz (therefore, it was not necessary to decimate the data). The raw data were then subjected to de-averaging (constant detrend) and filtered with a 4th order bandpass Butterworth filter, with cut-off frequencies equal to 0.5 Hz and 15 Hz, respectively. Figure 10 depicts the filtered accelerations (one hour and 10 min) and their main frequency component, as evidenced in a Welch spectrum.

Similarly to the 2010 identification [3], the entire filtered signal, made up of the recordings of the three channels (two along the minor inertia axis, viz. y-axis, and one along the major inertia axis, viz. x-axis, of the lantern) was then divided into seven 10-min segments. For each segment, the dynamic identification was repeated to refine the estimates of the modal parameters. In this regard, the Stochastic Subspace Identification (SSI) algorithm #3 was used in conjunction with the weighting scheme given by Canonical Variate Analysis (CVA) [35]. Implementing the stabilization approach, the identifications were repeated between a

Fig. 9 Acquisition system and sensors installed on the top of the lantern (**a**), experimental setup layout (with the sensors in red) (**b**) and installation of the sensor on the lantern (**c**)
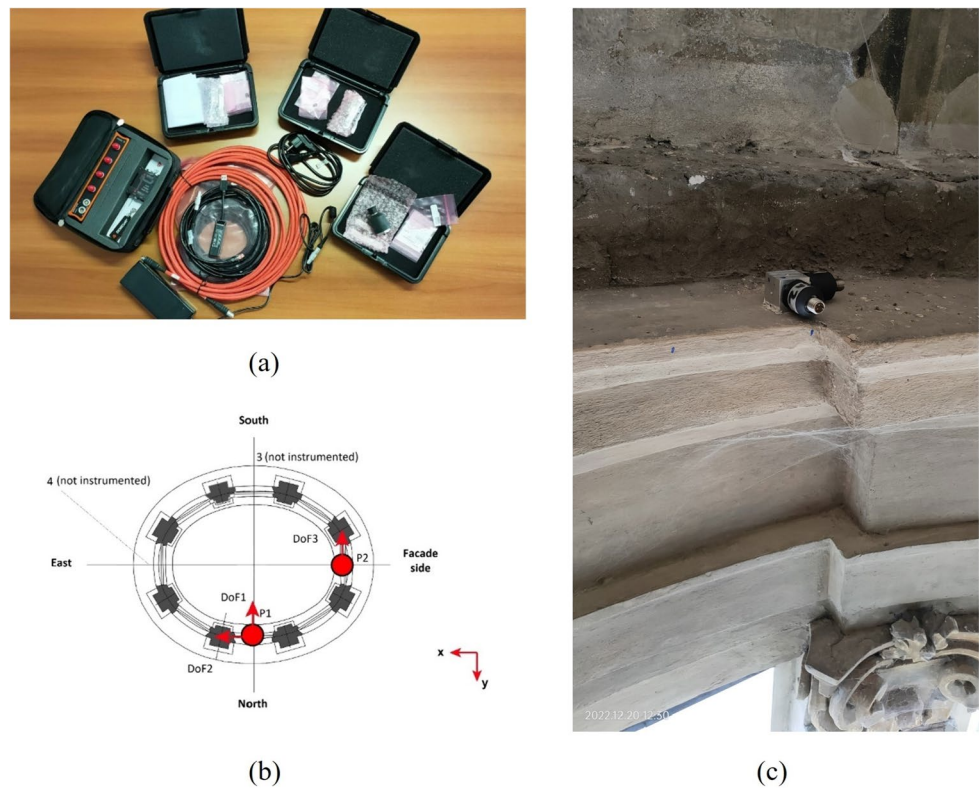
Table 4 Channel data of the experimental setup (*Degree of Freedom)

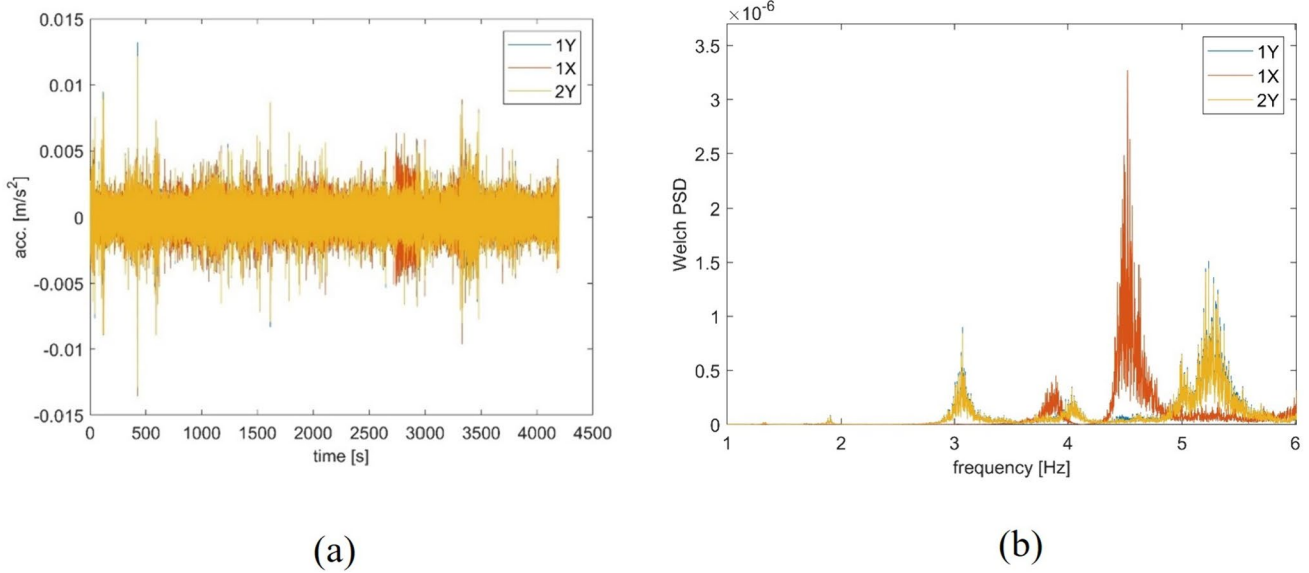| DoF*	Data	Channel	Sensor	Position	Direction	Name	Sign
1	Accel	2	2	1	Y	1Y	− 1
2	Accel	3	3	1	X	1X	1
3	Accel	4	4	2	Y	2Y	− 1

(a)

(b)

Fig. 10 Filtered structural accelerations (**a**), and Welch Power Spectral Density (PSD) (**b**)

minimum and maximum system order of 20 and 200, respectively, with a step increment of two orders. On the basis of a hard-criterion, only modes exhibiting a damping ratio between 0.5 and 6% were accepted. As far as the stabilization analysis is concerned, all the modes that showed a frequency deviation lower than 0.025 Hz, a damping deviation lower than 20%, and MAC (Modal Assurance Criterion) higher than 0.98 were considered as stable. A further cluster analysis was conducted focusing between 1 and 10 Hz, accepting a maximum difference between frequencies equal to 0.08 Hz for the definition of the cluster. The modal parameters identified correspond to the average value found within

the clusters. Finally, an operation of coupling and averaging of the results obtained from the seven identifications was carried out. This provided the modal parameters of the structure in terms of modal damping ratio, natural frequency and mode shape related to the diaphragmatic movements of the top part of the lantern. Figure 11 depicts the resulting stabilization and clustering diagram for the coupled identifications.

Similarly to the results and diagrams of the 2010 extensive campaign, six stable modes were detected at the frequencies reported in Table 5. In some acquisitions, some low frequency modes, ranging between 1.22 and 1.89 Hz, were also detected, and attributed to the
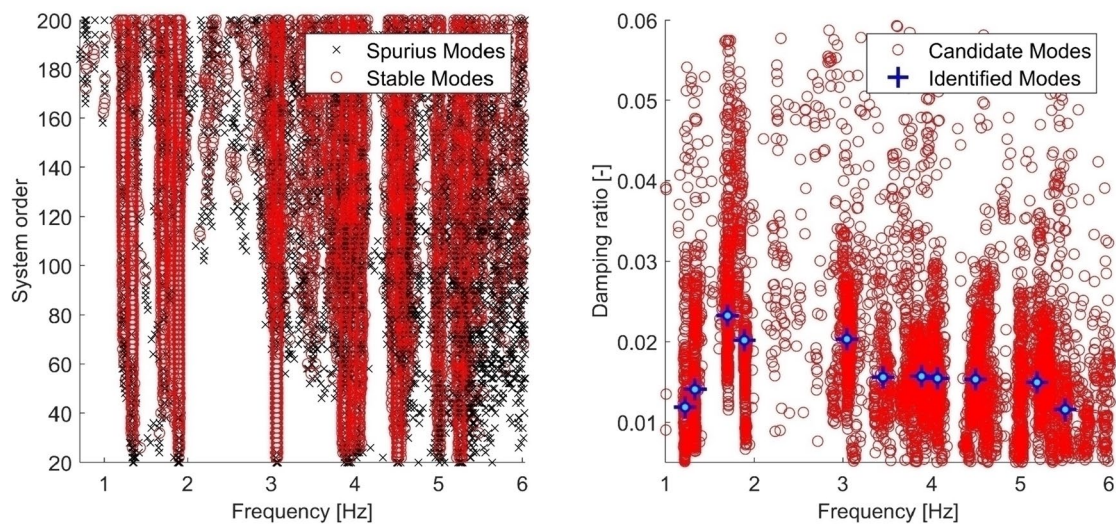

Fig. 11 SSI algorithm: stabilization (left) and clustering (right) diagrams

Table 5 Six identified natural frequencies, *f*, damping ratio, *ζ*, from 2022 campaign

Identifier	Description	f [Hz]	ζ [%]
1	Lantern moves transversally in y direction	3.05	2.00
2	The lantern moves mainly transversally in y direction with small longitudinal effects (*x* direction)	3.45	1.60
3	The lantern moves mainly transversally in y direction with smaller components in longitudinal direction (*x* direction)	4.06	1.50
4	The lantern moves mainly longitudinally in *x* direction with smaller components in transverse direction (*y* direction)	4.49	1.50
5	The lantern moves transversally in *y* direction, and very little in the longitudinal direction (*x* direction)	5.19	1.50
6	The lantern moves equally in the transverse and longitudinal directions (*x*- and *y* directions)	5.51	1.20
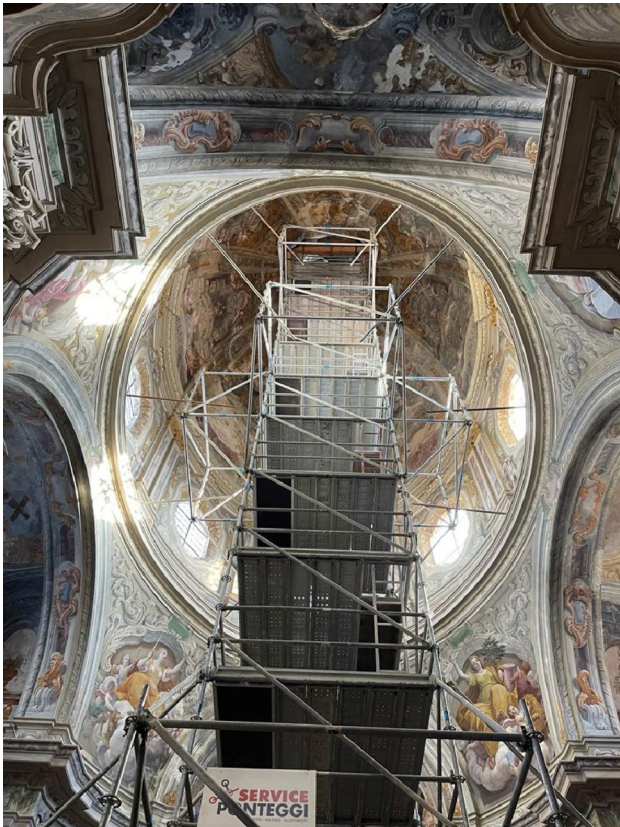
Fig. 12 Picture of the scaffolding

temporary scaffolding built inside the church to connect the lantern to the base for the ongoing restoration work on the frescoes. A separate discussion should be made for the newly detected frequency component at 3.88 Hz. To support these hypotheses, on 2023, June 19th a further dynamic experimental campaign was carried out to identify the scaffolding vibration modes. The scaffolding is depicted in Fig. 12.

A triaxial MEMS accelerometer was sequentially placed in three different positions on which scaffolding accelerations were acquired for a total duration of 200 s, with signals sampled at 400 Hz. The Fourier spectra of the acquisitions are shown in Fig. 13.

As a result of these acquisitions, it was possible to conclude that the modes identified between 1 and 2 Hz within the experimental campaign of December 2022 coincide with the modes identified for the scaffolding. Furthermore, no modes with a natural frequency of 3.88 Hz were identified, supporting the hypothesis that there is no correlation of this mode with the dynamic behaviour of the scaffolding. The six modes attributed to the church appear to be substantially consistent with the ones resulting from the 2010 campaign. Table 5, for completeness, also reports damping ratios, but it is known that the output-only methods lead to relatively large errors in the estimation of this parameter [34], and that a more reliable evaluation will result from the analysis of the historical series of permanent monitoring.

Comparing Table 1 and Table 5, one can observe a generally slight increase of the natural frequencies throughout the years, which is probably due to the local stiffening of the lantern and the façade, as well as oscillations due to Environmental and Operational Variations (EOVs).

4.3 Model updating

In this Section, the updating of the mechanical model described in Sect. 3.2 is presented. The FEM was tuned by exploiting the mode shapes and the natural frequencies deriving from the 2022 linear dynamic identification process. In particular, the frequencies at 3.05 Hz and 4.06 Hz, which are the ones corresponding to the bending mode shapes in the two transversal directions, were considered. Indeed, it was found a correspondence between these vibration modes and the modes obtained in the 2010 identification process. In general, model updating consists of modifying the characteristics of the materials by different attempts until a good correlation between the experimental and the numerical values is obtained. For each macro-element, the elastic modulus was varied to discrete values covering a fixed range in order to minimize the assumed cost function. The chosen objective function *J* modified by [39, 40] writes:
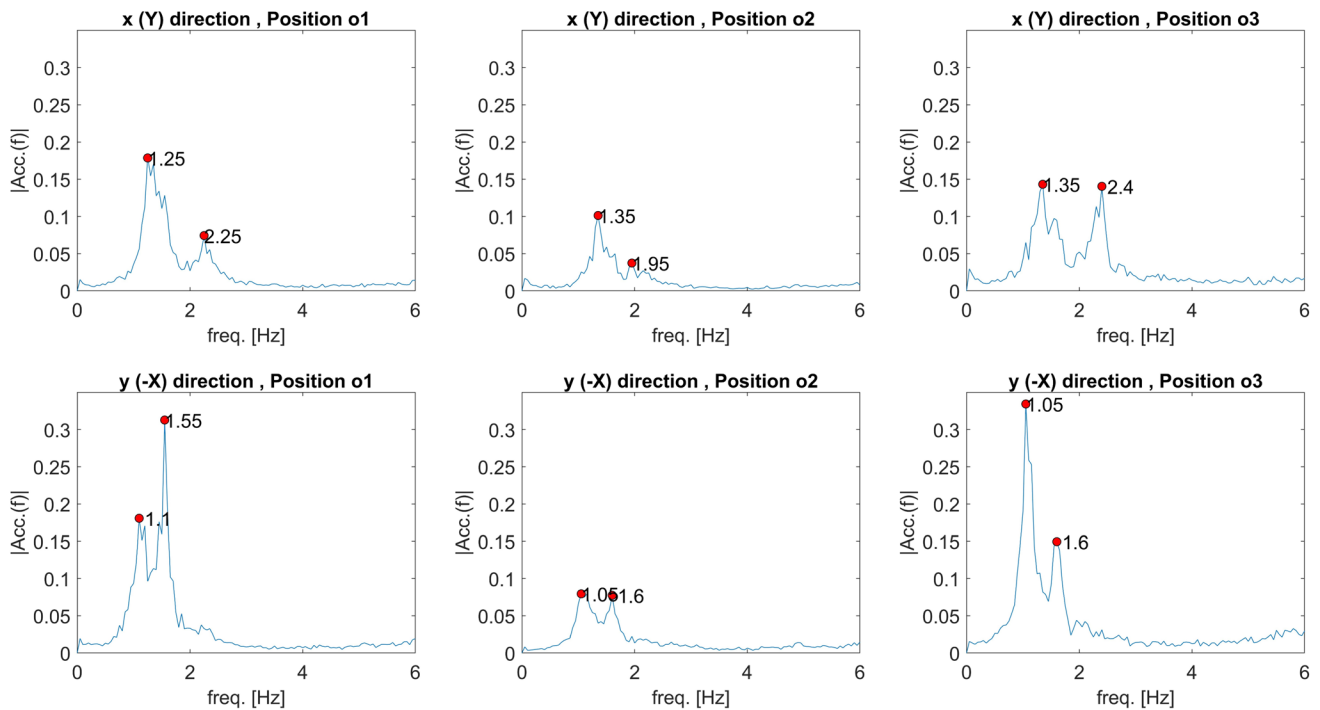
Fig. 13 Fourier spectra of the recorded accelerations of the scaffolding for sensor positioned in "o1", "o2" and "o3". X and Y define the global reference system direction, while x and y define the local reference system direction of the sensor

$$J = \sum_{j=1}^{m/2} \alpha_w \left| \frac{f_j^{id} - f_j}{f_j^{id}} \right| + \beta_w \left| \frac{1 - MAC_j}{1} \right| \qquad (1)$$

where m is the double of the modes number, jth denotes a generic mode, α_w and β_w are the weights of the residuals in frequency and mode shapes, respectively, f_j^{id} is the jth identified natural frequency, f_j is the jth predicted natural frequency, and MAC_j is the jth MAC (Modal Assurance Criterion) between the jth identified mode shape and the coupled predicted mode shape. The weights α_w and β_w can be assumed between 0 and 1, and then determined with a trial-and-error procedure [40].

In general, the number and type of parameters involved in the updating should be appropriately chosen: the number of parameters should not be too low or too high, and they should be physically meaningful [41]. In this case, three mechanical parameters could have been potentially calibrated: the elastic modulus, the Poisson's ratio, and the density. A preliminary sensitivity analysis was carried out before the whole process in order to choose the most suitable parameters for the updating [42, 43]. The preliminary local sensitivity analysis highlighted that the highest contribution to the variance of the natural frequencies predicted by the model is given by the basement. On the other hand, the elastic modulus of the external walls linking the church to the choir and to the adjacent buildings

did not seem to significantly affect the modal properties of the structure. The analysis confirmed the elastic modulus as the most sensitive parameter for the considered modes. Also, in the model updating carried out after the experimental campaign of 2010, the density resulted to be identical for all the seven materials, since the real variation of that parameter on the structure was lower than the discretization range used to evaluate it within the model. The same reasoning was applied to the Poisson's ratio, which resulted to be uniform over the whole structure.

Given these considerations, the density and the Poisson's ratio were not considered as parameters to be updated, and only the elastic modulus was varied in a predefined range. This range of variation was assumed based on the current Italian standards [38]. In greater detail, it was assumed a range between 600 and 1800 MPa in the case of the lantern, of the façade and drum − dome system, and a range between 1200 and 5600 MPa in the case of the base and the external walls. Consequently, the elastic modulus of the different macro-elements was calibrated in subsequent steps, provided by the sensitivity analysis, mitigating in this way the risk to be trapped in local minima. This approach resulted in a guided calibration of the model. A total number of 5 parameters have been updated. The initial value was chosen equal for each parameter (viz., the elastic modulus of each of the 5 macro-elements) and corresponded to 2500 MPa.

In a first step, all parameters were varied in the predefined ranges to identify their most plausible physical range of variation. However, a too high number of parameters could lead to inaccurate results. This gathered further steps of calibration to ensure the validity of the found values of the elastic modulus: first, the parameters associated to the base, the drum − dome system, and the external walls were calibrated, and, in a second step, the lantern and the façade were considered. This choice was made due to the high influence of the lantern and the façade on local behaviours rather than the global one and, therefore, to the high uncertainty of these parameters to be calibrated with global quantities. Eventually, the fine tuning of the parameters was carried out, within a range of variation of 15–20%, based on existing mechanical tests. The values of the elastic modulus obtained from the calibration process can be found in Fig. 14.

From Fig. 14 it is observable that the basement, the drum − dome system, and the lantern present values of the elastic modulus which are progressively lower. Moreover, the updated value of the elastic modulus of the basement is in line with the one resulting from the mechanical tests presented in Table 3. The elastic modulus of the façade, which represents the other vulnerable element of the church, confirms that it has substantially different values from the body of the church, as also highlighted by the model updating process carried out in 2010. This seems to be mainly ascribed to the material, as all surveys carried out after the installation of the intervention described in Sect. 3.1 highlighted a good connection between the façade and the rest of the church. Moreover, the presence of a regular masonry texture and the absence of cracks at the intersections were confirmed. Finally, the external walls present a very high value of the elastic modulus. However, as underlined by the sensitivity analysis, any value virtually taken by this
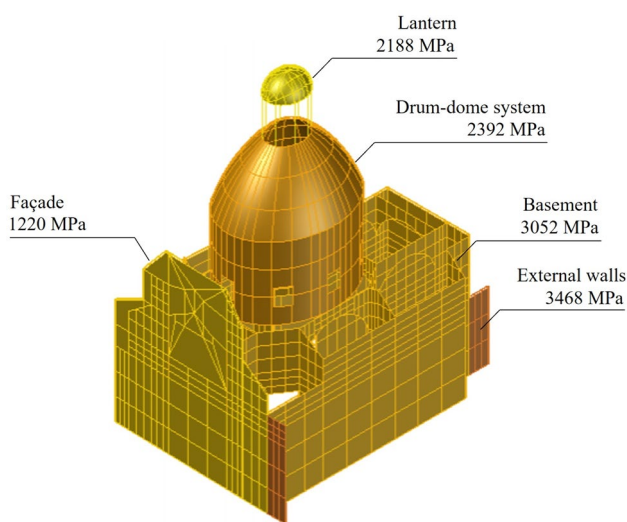
parameter would result in an unchanged modal behaviour. Even so, it should be noted that its value is close to that of the basement, although no relationship has been established between the two parameters during calibration. For what concerns the natural frequencies of the system, which are reported in Table 6, it is observable a slight discrepancy in the values between the results of the identification process and the ones of the updating, however in line with expectations given the simplifications introduced, for example, on the choir. The same discrepancy can be found also in the frequencies found after the experimental campaign of 2010 (see Table 2).

5 Checks on the effectiveness of the seismic upgrading interventions

5.1 Verification of the models

Updated models, even when they present small discrepancies with respect to experimental measurements, might be inconsistent and need to be verified. In order to accomplish this, the interventions were removed and the modes of the two models, viz. the updated model of 2010 and the updated model of 2022 without interventions, were compared in terms of natural frequencies in Table 7 and mode shapes in Fig. 15.

The comparison between the two models does not lead to striking differences, except for the mode shapes that tend to be more uniform in the 2022 model. Furthermore, even the frequencies have discrepancies comparable to those obtained with respect to the experimental data, highlighting that the numerical uncertainties due to processing and model discrepancy are comparable to the observation errors.

A further observation concerns the local mode of the façade that was not acquired in the 2010 campaign. In the updated model with interventions, this mode stands at a frequency that is incremented from the one without interventions, 2.87 Hz, to 3.58 Hz, this being consistent both with the new mode identified at 3.88 Hz and with the reduction of the overhang due to the contrast of the metal frame. At any rate, verification of local modes will be possible when
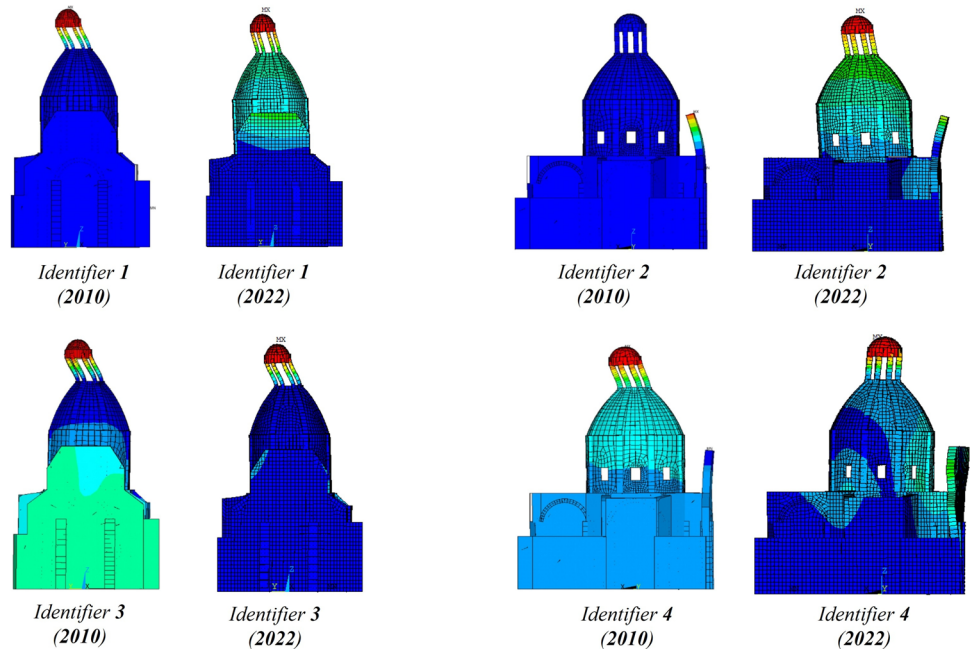

Fig. 14 Updated values of the elastic modulus of the macro-elements

Table 6 Results of the calibration process: frequencies obtained from the FE model vs. frequencies obtained from the dynamic identification of the 2022 campaign

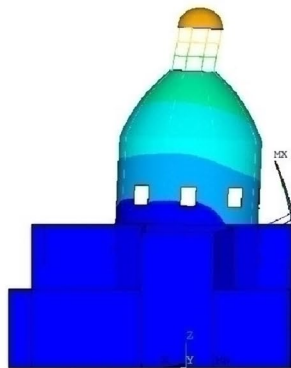| Identifier	Mode number in FEM (2022)	Freq. FEM (2022) [Hz]	Freq. ID. (2022) [Hz]	ΔF [%]
1	1	2.93	3.05	3.93
2	2	3.14	3.45	8.98
3	4	4.12	4.06	− 1.48
4	5	4.81	4.49	− 7.13

Table 7 Comparison between the frequencies of the FEM resulting from the old and the new updating: 2010 testing campaign and 2022 testing campaign/without interventions, respectively

Identifier	Mode number in FEM (2010)	Freq. FEM (2010) [Hz]	Mode number in FEM (2022)	Freq. FEM (2022) [Hz]	ΔF_{FEM} [%]
1	1	2.94	2	2.91	− 1.03
2	2	3.53	3	3.46	− 2.02
3	3	4.29	4	3.91	− 9.72
4	4	4.30	5	4.49	4.23

Fig. 15 Comparison between the mode shapes of the FEM resulting from the old updating and the new updating, corresponding to 2010 testing campaign and 2022 testing campaign (no interventions), respectively

Identifier 1 (2010) *Identifier 1 (2022)* *Identifier 2 (2010)* *Identifier 2 (2022)*

Identifier 3 (2010) *Identifier 3 (2022)* *Identifier 4 (2010)* *Identifier 4 (2022)*
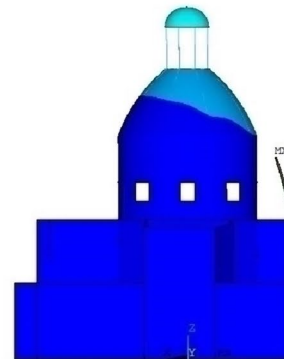

Fig. 16 Mode shape of mode at 3.88 Hz predicted by the new calibrated FE model with (left) and without (right) retrofitting interventions

the definitive permanent monitoring system is installed. Figure 16 depicts the comparison between the mode shape of the mode at 3.88 Hz predicted by the new calibrated FE model with and without upgrading interventions, respectively.

5.2 Effects of the interventions on the vibration modes of the calibrated model

Once the reliability of the 2022 FE model has been verified, the assessment of the effectiveness of the interventions was
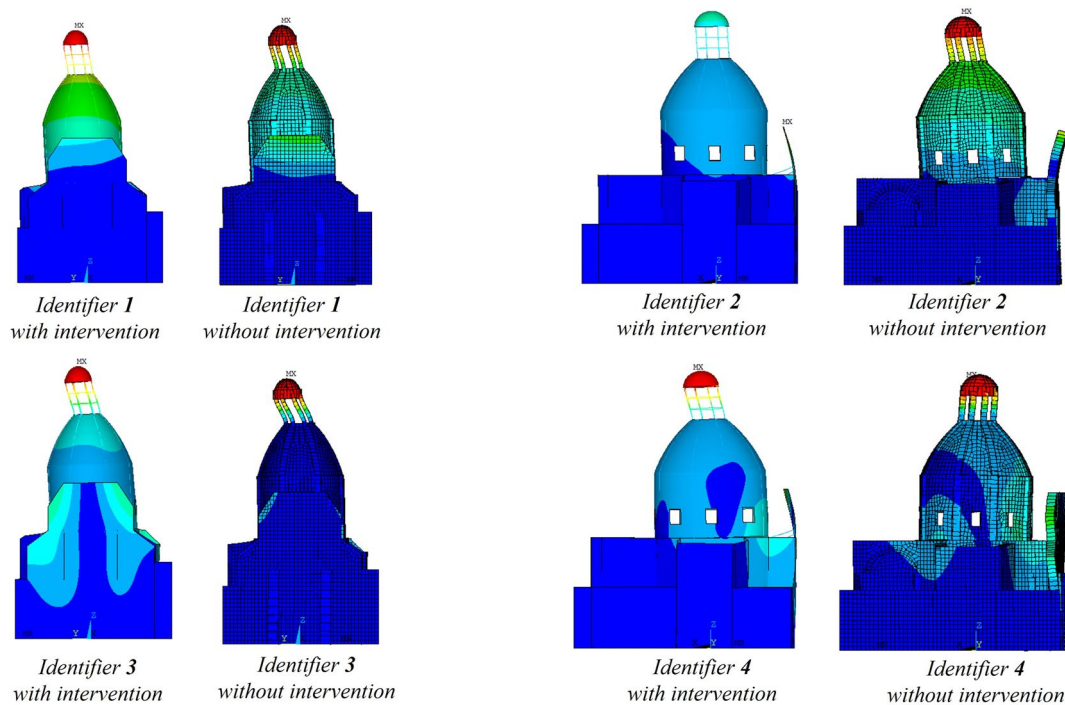
Fig. 17 Comparison between the mode shapes of the FEM before and after the interventions by employing the 2022 model without and with the interventions

Table 8 Comparison between the frequencies of the FEM before and after the interventions by employing the 2022 model without and with the interventions

Identifier	Mode number in FEM	Freq. FEM without intervention [Hz]	Mode number in FEM	Freq. FEM with intervention (2022) [Hz]	ΔF_{FEM} [%]
1	2	2.91	1	2.93	+ 0.68
2	3	3.46	2	3.14	− 9.25
3	4	3.91	4	4.12	+ 5.37
4	5	4.49	5	4.81	+ 7.12

conducted by exploiting it. Again, the mode shapes and the natural frequencies of the 2022 model, with and without intervention, were extrapolated. Figure 17 reports the mode shapes of the church in the two cases, while in Table 8 the natural frequencies can be found.

As can be seen in Fig. 17, the mode shapes of the numerical model did not change significantly from the pre-intervention to the post-intervention situation. This is an expected finding since interventions such as the ones carried out on this church do not affect the mass and/or the stiffness like other techniques. From Table 8, it can be observed that the modes of the two models are consistent, without any inversion of modes. However, a small discrepancy involving the additional mode identified at 3.88 Hz (see Fig. 16 for clarification) can be observed: on the one hand, in the case of the model without intervention, it corresponds to the first numerical mode, while in the case of the model with interventions, it corresponds to the third numerical mode. This

discrepancy can be attributed to the fact that this mode probably arises with strengthening interventions.

5.3 Environmental and operational variations effects

The paper critically analysed the differences between the modal parameters obtained in the 2010 experimental campaign, when a seismic retrofitting system had not yet been installed on the structure, and the dynamic identifications of 2022. The results of the study show a slight increase in natural frequencies of the system, on average equal to 2%. However, in 2010 the dynamic tests were carried out at the end of September, with an average ambient temperature of 20 °C. On the contrary, the dynamic identifications of 2022 reported in this work refer to the end of December, when the average temperatures were around 6 °C. In order to better understand the nature of the variation of the modal

Table 9 Six main natural frequencies within the identification campaigns (2010, 2022, and 2023)

Identifier	Frequency 2010 [Hz]	Frequency 2022 [Hz]	Frequency 2023 [Hz]
1	3.03	3.05	3.07
2	3.33	3.45	3.42
3	3.97	4.06	4.08
4	4.4	4.49	4.43
5	5.11	5.19	4.97
6	5.39	5.51	5.31

Table 10 Comparison between the six main natural frequencies within the identification campaigns (2010, 2022, and 2023)

Identifier	Difference 2022–2010 [%]	Difference 2023–2022 [%]	Difference 2023–2010 [%]
1	0.66	0.66	1.32
2	3.60	− 0.87	2.70
3	2.27	0.49	2.77
4	2.05	− 1.34	0.68
5	1.57	− 4.24	− 2.74
6	2.23	− 3.63	− 1.48
Average normalized difference [%]	+ 2.06	− 1.49	+ 0.54

behaviour of the system, a further dynamic identification with the data of 2023, March 11 (02:00 pm) has been carried out. On this date, the average air temperatures stood at the value recorded in the 2010 tests, i.e., 20 °C. The results of the comparison between the experimental campaigns, in terms of identified natural frequency, are reported in Table 9 and Table 10. It is worth noting that the comparison is made on the main global modes, the classification of which was made possible by the extensive campaign conducted in 2010 on the entire body of the structure [3]. Some local modes can in fact be easily discriminated in frequency using the FEM calibrated on the basis of the first campaign.

From the results reported in Table 9 and Table 10, it is possible to draw some preliminary conclusions, which call for further validation following an extensive study on the variation of the modal parameters during the data acquisition period December 2022 − March 2023 (which goes beyond the scope of this paper). The comparison between the identifications of 2022 and 2010 highlights that the presence of seismic retrofitting interventions, together with a decrease in temperature of 14 °C, leads to an increase in dynamic stiffness (i.e., natural frequencies) of about 2%. On the contrary, the only increase in temperature (of about 14 °C) that can be appreciated by comparing the identifications of 2022 and 2023 (in both cases, the seismic retrofitting

system is present) leads to a decrease in dynamic stiffness of approximately 1.5%. Finally, comparing the identifications of 2010 with those of 2023 (i.e., same ambient temperature but absence of the retrofitting system in the first case) one can note an increase of 0.55% in the frequencies of the global modes. On local modes, for example, the façade, the difference could be much more pronounced.

From these considerations, it is possible to conclude, in the first instance, and assuming a linear behaviour of the frequencies for temperatures between 6 and 20 °C, that the seismic retrofitting interventions show a small but still appreciable effect in terms of increased global stiffness under ambient vibrations. On the other hand, the variations due to the environmental variables (in this case synthesized in thermal variations) are about three times greater, so they must be taken into account by any vibration-based SHM protocol, e.g., evaluating seasonal trends or resorting to cointegration techniques [44].

6 Conclusions

The preservation of the built environment makes it mandatory to intervene structurally on structures damaged or degraded over time. For monumental buildings, the corroboration of a mechanical model can be helpful in limiting invasive interventions, as was done in the case of the seismic upgrading of the church of Santa Caterina in Casale Monferrato. In the paper, the authors valued the use of operational modal analysis and computational modelling in order to detect variations in the dynamic behaviour caused by the installation of seismic retrofitting systems on two components of the church: the lantern and the façade. In addition, the dynamic behaviour of the church was investigated on updated FE models in order to design a permanent vibration-based SHM system and define future monitoring protocols. The main conclusions of the work are summarized hereinafter:

- Corroborated models can be employed for identifying damage mechanisms on architectural heritage structures, and, as a consequence, for targeting the design of non-invasive interventions on their most vulnerable elements, and to verify their effectiveness, as demonstrated by the application to the Santa Caterina church in Casale Monferrato, Italy.
- The main natural frequencies of the structure have undergone a slight increase (1–3%) compared to the values identified in 2010, indicating the effectiveness of the interventions. However, a validation of this hypothesis will only be possible following dynamic identification operations repeated over time, in order to take into account the possible oscillations due to thermal cycles.

- The dynamic test campaign conducted after the seismic upgrading has highlighted the appearance of a mode at 3.88 Hz, which mainly activates the façade and the lantern in the longitudinal direction.
- The calibrated models highlight a low stiffness value of the façade, if compared with the stiffness of the materials constituting the other macro-components of the church. This indicates a potential degradation of this macro-component and confirms the validity of the design solutions and, in general, the importance of using corroborated mechanical models for the conservation of architectural heritage buildings.

Data availability Data employed in the current study are available from the corresponding author on reasonable request.

Declarations

Conflict of interest No potential conflict of interest was reported by the author(s).

References

1. Charter I (2003) Principles for the analysis, conservation and structural restoration of architectural heritage. Proceed ICOMOS 14th Gen Assem Vic Falls, Vic Falls, Zimb 27–31
2. Farrar CR, Worden K (2007) An introduction to structural health monitoring. Phil Trans R Soc A: Math, Phys Eng Sci 365:303–315
3. Ceravolo R, Pistone G, Fragonara LZ, Massetto S, Abbiati G (2016) Vibration-based monitoring and diagnosis of cultural heritage: a methodological discussion in three examples. Int J Archit Herit 10:375–395. https://doi.org/10.1080/15583058.2013.850554
4. Ceravolo R, De Lucia G, Lenticchia E, Miraglia G (2019) Seismic structural health monitoring of cultural heritage structures. In: Limongelli MP, Çelebi M (eds) Seismic structural health monitoring. Springer, Cham, pp 51–85
5. De Stefano A, Matta E, Clemente P (2016) Structural health monitoring of historical heritage in Italy: some relevant experiences. J Civ Struct Heal Monit 6:83–106
6. Casarin F, Modena C (2008) Seismic assessment of complex historical buildings: application to Reggio Emilia Cathedral, Italy. Int J Archit Herit 2:304–327
7. Ramos LF, Marques L, Lourenço PB, De Roeck G, Campos-Costa A, Roque J (2010) Monitoring historical masonry structures with operational modal analysis: two case studies. Mech Syst Signal Process 24:1291–1305
8. Modena C, Lorenzoni F, Caldon M, da Porto F (2016) Structural health monitoring: a tool for managing risks in sub-standard conditions. J Civ Struct Heal Monit 6:365–375
9. Gentile C, Ruccolo A, Canali F (2019) Continuous monitoring of the Milan Cathedral: dynamic characteristics and vibration-based SHM. J Civ Struct Heal Monit 9:671–688
10. Ormando C, Raeisi F, Clemente P, Mufti A (2021) The SHM as higher level inspection in the evaluation of structures. International Conference of the European Association on Quality Control of Bridges and Structures. Springer International Publishing, Cham, pp 452–461
11. Saisi A, Gentile C, Ruccolo A (2018) Continuous monitoring of a challenging heritage tower in Monza, Italy. J Civ Struct Heal Monit 8:77–90
12. Miraglia G, Lenticchia E, Ceravolo R, Betti R (2019) Synergistic and combinatorial optimization of finite element models for monitored buildings. Struct Control Health Monit 26:e2403
13. Cattari S, Degli Abbati S, Ottonelli D, Marano C, Camata G, Spacone E, Da Porto F, Modena C, Lorenzoni F, Magenes G et al (2019) Discussion on data recorded by the Italian structural seismic monitoring network on three masonry structures hit by the 2016–2017 Central Italy earthquake. Proc COMPDYN 1:1889–1906
14. Giordano PF, Ubertini F, Cavalagli N, Kita A, Masciotta MG (2020) Four years of structural health monitoring of the San Pietro bell tower in Perugia, Italy: two years before the earthquake versus two years after. Int J Mason Res Innov 5:445–467
15. Russo S (2013) On the monitoring of historic Anime Sante church damaged by earthquake in L'Aquila. Struct Control Health Monit 20:1226–1239
16. Ubertini F, Cavalagli N, Kita A, Comanducci G (2018) Assessment of a monumental masonry bell-tower after 2016 Central Italy seismic sequence by long-term SHM. Bull Earthq Eng 16:775–801
17. Sarhosis V, Dais D, Smyrou E, Bal IE, Drougkas A (2021) Quantification of damage evolution in masonry walls subjected to induced seismicity. Eng Struct 243:112529
18. Ceravolo R, Coletta G, Miraglia G, Palma F (2021) Statistical correlation between environmental time series and data from long-term monitoring of buildings. Mech Syst Signal Process 152:107460
19. Gentile C, Guidobaldi M, Saisi A (2016) One-year dynamic monitoring of a historic tower: damage detection under changing environment. Meccanica 51:2873–2889. https://doi.org/10.1007/s11012-016-0482-3
20. Mesquita E, Arêde A, Silva R, Rocha P, Gomes A, Pinto N, Antunes P, Varum H (2017) Structural health monitoring of the retrofitting process, characterization and reliability analysis of a masonry heritage construction. J Civ Struct Heal Monit 7:405–428

21. Clemente P (2017) Seismic isolation: past, present and the importance of SHM for the future. J Civ Struct Heal Monit 7:217–231
22. Zanotti Fragonara L, Boscato G, Ceravolo R, Russo S, Ientile S, Pecorelli ML, Quattrone A (2017) Dynamic investigation on the Mirandola bell tower in post-earthquake scenarios. Bull Earthq Eng 15:313–337
23. Masciotta M-G, Ramos LF, Lourenço PB (2017) The importance of structural monitoring as a diagnosis and control tool in the restoration process of heritage structures: a case study in Portugal. J Cult Herit 27:36–47
24. Roca P, Cervera M, Gariup G, Pela L (2010) Structural analysis of masonry historical constructions. classical and advanced approaches. Arch Comput Methods Eng 17:299–325
25. Osmancikli G, Uçak Ş, Turan FN, Türker T, Bayraktar A (2012) Investigation of restoration effects on the dynamic characteristics of the Hagia Sophia bell-tower by ambient vibration test. Constr Build Mater 29:564–572
26. Yanık Y, Aymelek A, Çalık İ, Türker T (2022) Vibration testing and performance evaluation of Hagia Sophia bell tower after recent restoration. Constr Build Mater 347:128617
27. Mirtaheri M, Abbasi A, Salari N (2017) A seismic behavior and rehabilitation of the historic masonry minaret by experimental and numerical methods
28. Bayraktar A, Çalik İ, Türker T, Ashour A (2018) Restoration effects on experimental dynamic characteristics of masonry stone minarets. Mater Struct 51:1–14
29. Romero M, Pachón P, Compán V, Cámara M, Pinto F (2018) Operational modal analysis: a tool for assessing changes on structural health state of historical constructions after consolidation and reinforcement works—Jura Chapel (Jerez de la Frontera, Spain). Shock Vib 2018:1–12
30. Di Primio A, Fiorini N, Spina D, Valente C, Vasta M (2021) Ambient vibrations for the assessment of the strengthening intervention of a masonry barrel vault. Struct Health Monit 20:1312–1330
31. Çalık İ, Bayraktar A, Türker T, Karadeniz H (2014) Structural dynamic identification of a damaged and restored masonry vault using Ambient Vibrations. Measurement 55:462–472
32. Gentile C, Poggi C, Ruccolo A, Vasic M (2019) Vibration-based assessment of the tensile force in the tie-rods of the milan cathedral. Int J Archit Herit 13:411–424. https://doi.org/10.1080/15583058.2018.1563235
33. Consiglio superiore dei lavori pubblici (2011) Linee Guida per la valutazione e riduzione del rischio sismico del patrimonio culturale - allineamento alle nuove Norme tecniche per le costruzioni
34. Ceravolo R, Abbiati G (2013) Time domain identification of structures: comparative analysis of output-only methods. J Eng Mech 139:537–544
35. Van Overschee P, De Moor BL (2012) Subspace identification for linear systems: Theory—Implementation—Applications. Springer Science\& Business Media
36. Larimore WE (1990) Canonical variate analysis in identification, filtering, and adaptive control. In: 29th IEEE Conference on Decision and control. pp 596–604
37. Foppoli Moretta e Associati (2012) Relazione prove non distruttive su Santa Caterina a Casale Monferrato (in italian)
38. Ministero delle Infrastrutture e dei Trasporti (2018) Aggiornamento delle «Norme tecniche per le costruzioni»
39. Moller PW, Friberg O (1998) Updating large finite element models in structural dynamics. AIAA J 36:1861–1868
40. Merce RN, Doz GN, de Brito JLV, Macdonald J, Friswell MI (2007) Finite element model updating of a suspension bridge using ansys software. In: Design and Optimization Symposium
41. Friswell M, Mottershead JE (1995) Finite element model updating in structural dynamics. Springer Science & Business Media, Dordrecht
42. Mottershead JE, Link M, Friswell MI (2011) The sensitivity method in finite element model updating: a tutorial. Mech Syst Signal Process 25:2275–2296
43. Boscato G, Russo S, Ceravolo R, Fragonara LZ (2015) Global sensitivity-based model updating for heritage structures. Comput-Aided Civ Infrastruct Eng 30:620–635
44. Coletta G, Miraglia G, Pecorelli M, Ceravolo R, Cross E, Surace C, Worden K (2019) Use of the cointegration strategies to remove environmental effects from data acquired on historical buildings. Eng Struct 183:1014–1026